

# The Characteristics of Raindrop Size Distribution and Drop Shape Relation in Typhoon Systems from 2D-Video Disdrometer and NCU C-Band Polarimetric Radar

Wei-Yu Chang   Tai-Chi Chen Wang   Pay-Liam Lin  
National Central University

## 1. Introduction :

The raindrop size distribution (DSD) and the drop shape relation (DSR) have great variation in different types of rainfall condition. The DSDs and DSRs can determine not only the different moment of rainfall integral parameters but also the measurements of polarimetric radar. Through the calculation from DSDs, the coefficient  $N_0$ ,  $\mu$ ,  $\Lambda$  of Gamma distribution can be retrieved. (Ulbrich 1983) The median volume diameter ( $D_0$ ), mass-weighted diameter ( $D_m$ ) and the normalized intercept ( $N_w$ ) were also derived through the coefficient  $N_0$ ,  $\mu$ ,  $\Lambda$ . From year 2001 to 2005, we had analyzed five years DSDs data from 2d-video disdrometer. The characteristics of DSDs and DSRs in 13 typhoon systems were obtained through statistics.

## 2. DSDs from 2d-video disdrometer :

The vertical profile of reflectivity and the rainfall rate indicated three different types of precipitation systems: the weak stratiform, stratiform and the convection systems. (Fig.1) The DSDs in weak stratiform systems had small maximum diameter (2~3mm) and relatively fewer small to median diameter of raindrops with lower reflectivity (less than 25 dBZ), the stratiform systems had bigger maximum diameter (2.5~3.5mm) and relatively more small to median diameter of raindrops with higher reflectivity (30~40 dBZ), and the convection systems had the biggest maximum diameter (3.5~4.5mm) and the most small to median diameter of raindrops with distinct strong reflectivity column.

Thus, the scatter-plot of  $D_m$  and the log-scale  $N_w$  were used to illustrate the characteristics of DSDs in

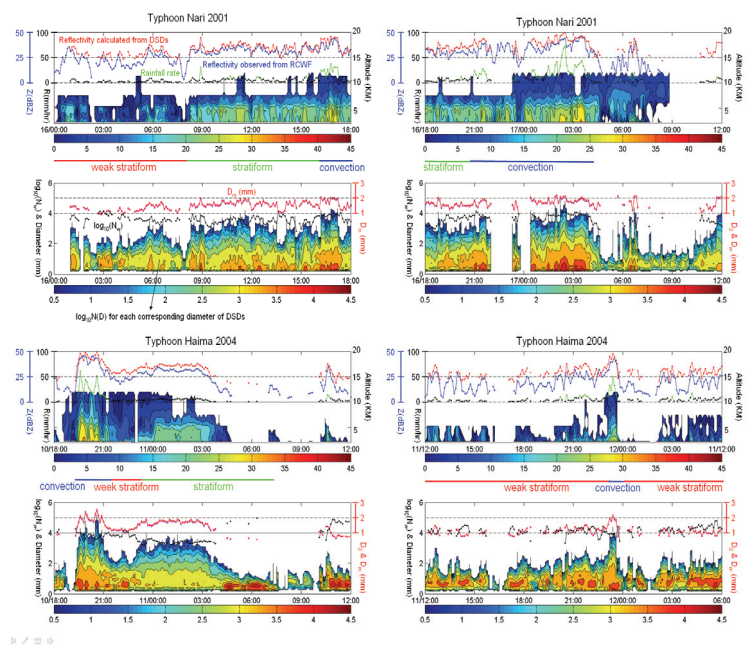


Fig.1: The time series of rainfall rate (green line), reflectivity calculated from DSDs (red line) and observed from RCWF (blue line) and vertical profile of reflectivity (color shaded) in (a), (b), (e) and (f). The  $D_m$  (red line),  $\log_{10}(N_w)$  (black line) and DSDs (color shaded) in (b), (d), (g), and (h).

different rainfall rate in typhoon systems. In Fig.2, the average  $D_m$  and log-scale  $N_w$  were calculated for each 10 mm/hr rainfall rate. For the rainfall rate less than 10 mm/hr which indicating stratiform precipitation, showed that the stratiform precipitation in typhoon Haima (Nari) had higher (lower)  $N_w$  and smaller (bigger)  $D_m$ . On the other hand, in the convection precipitation (rainfall rate greater than 10 m/hr), the  $D_m$  and  $N_w$  of DSDs in typhoon Haima 2004 showed higher  $N_w$  and smaller  $D_m$

for each corresponding rainfall rate comparing to typhoon Nari 2001. And the  $D_m$  increased with the increasing rainfall rate as typhoon Nari 2001, however, the  $D_m$  remained about 2.2 mm when rainfall rate greater 50 mm/hr. The results showed that the heavy precipitations were mainly composed by the concentration of raindrops of DSDs rather than the giant diameter of raindrops both in typhoon Nari and Haima. Consequently, the balance of the microphysical process of collision-coalescence and breakup in typhoon system may cause the unique constrained  $D_m$  value in heavy precipitation.

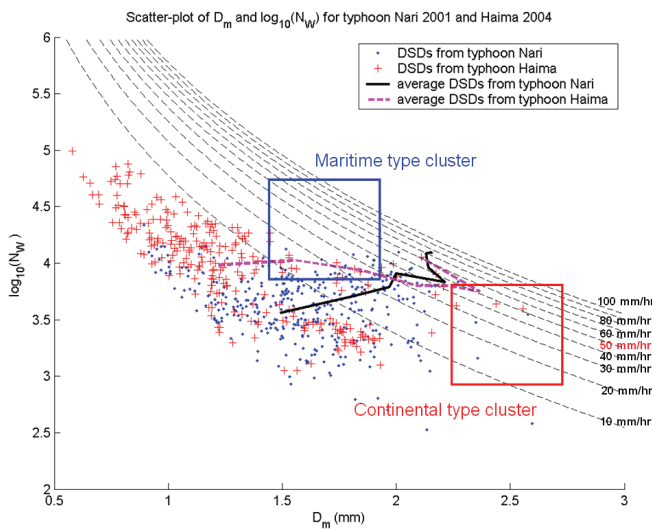


Fig. 2: The scatter-plot of  $D_m$  and  $\log_{10}(N_w)$  for typhoon Nari 2001 and Haima 2004 with the average  $D_m$  and  $\log_{10}(N_w)$  for each 10 mm/hr rainfall rate (Nari 2001: black line, Haima 2004: pink dash line). The black dash line represents the rainfall rate from 10 to 100 mm/hr, blue (red) square represents the maritime (continental) type cluster from Bringi et al. 2003, respectively.

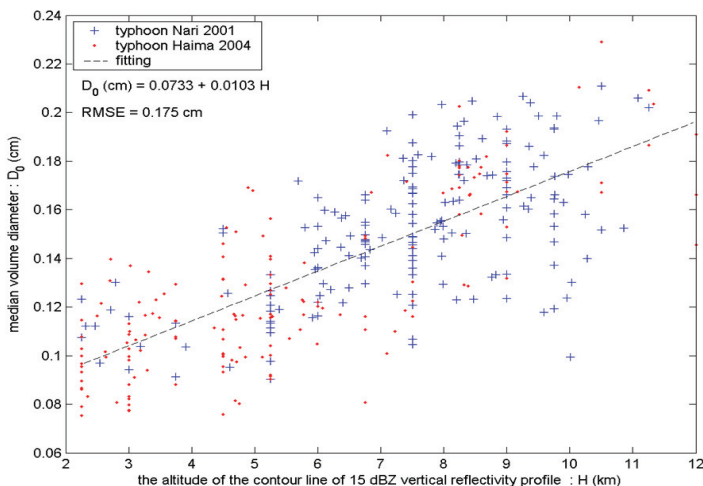


Fig. 3: The scatter-plot of  $D_0$  and the altitude of 15 dBZ contour line of vertical reflectivity. The data from typhoon Nari and Haima are red dots and blue cross, respectively. The black dash line represents the best linear fitting of  $D_0$  and the altitude of 15 dBZ contour line of vertical reflectivity.

According to the DSDs and RCWF observed reflectivity profile data, we found that the depth of the system had a good correlation with the median volume diameter ( $D_0$ ) of DSDs. In Fig. 3, the altitude of 15 dBZ contour lines ( $H$ ) were used as an indicator to represent the depth of the systems, which had a good linear relation with  $D_0$ . The  $D_0$  increased with the increasing of the altitude of 15 dBZ contour lines. Stronger convection systems may provide more collision-coalescence or the melting snow-flaks and graupel from higher altitude maybe the reasons for this linear relation.

### 3. DSDs retrieval from NCU C-Band polarimetric radar :

The DSDs retrieval from polarimetric radar has been archived by using constrain-gamma method ( $\mu$ - $\Lambda$  relation) and polarimetric measurements: differential reflectivity ( $Z_{DR}$ ) by Zhang et al. 2001. However, the accuracy of the  $\mu$ - $\Lambda$  relation and the drop shape relation (DSR) of raindrops will highly effect the results from the retrieval of DSDs from polarimetric radar, thus, it's important to understand the  $\mu$ - $\Lambda$  relation and the DSR in typhoon systems first.

#### (1) $\mu$ - $\Lambda$ relation in typhoon systems:

In Fig. 4, the scatter-plot of  $\mu$  and  $\Lambda$  from 13 typhoon systems showed totally different relation comparing to the results of Brandes et al. 2002. The results suggest that  $\mu$ - $\Lambda$  relation for typhoon systems were necessary, thus, the  $\mu$ - $\Lambda$  relation for typhoon systems were derived to replace the one from Brandes 2004 et al..

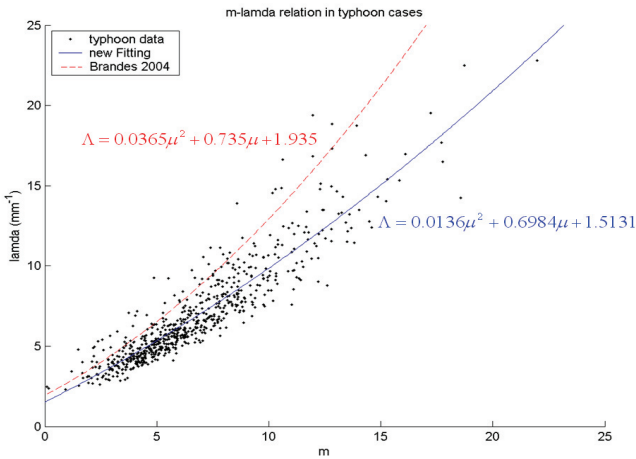


Fig. 4: The scatter-plot of  $\mu$  and  $\Lambda$  from 13 typhoon systems (black dots), red dash line was from Brandes et al. 2004 and the blue line was the new  $\mu$ - $\Lambda$  relation for typhoon systems.

(2) DSR of typhoon systems:

In Fig. 5, the axis ratio from 2d-video disdrometer of typhoon systems (Fig. 5(a)) showed that the shape of raindrops were slightly more spherical comparing with non-typhoon systems in low horizontal wind (0~1 m/s) and rainfall rate (0~2 mm/hr) condition (Fig. 5(b)) in the same successive observation period. Both the axis ratios were also compared with Brandes et al. 2002 and Thurai et al. 2005, the results indicate that the axis ratio in non-typhoon was very similar to the previous two research, but relatively more spherical in typhoon system. The comparisons reveal that the instrumental effect was limited and acceptable.

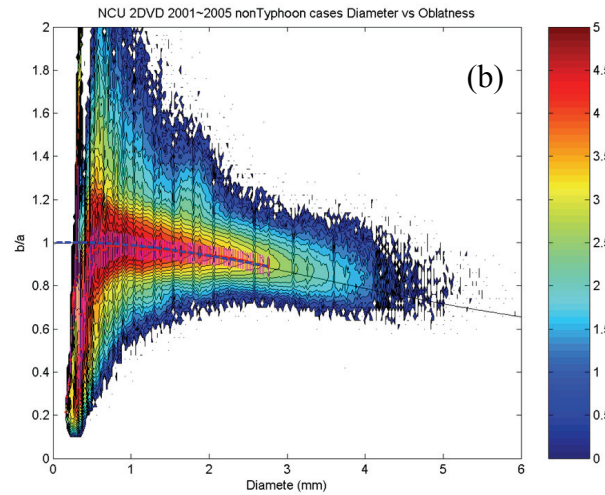
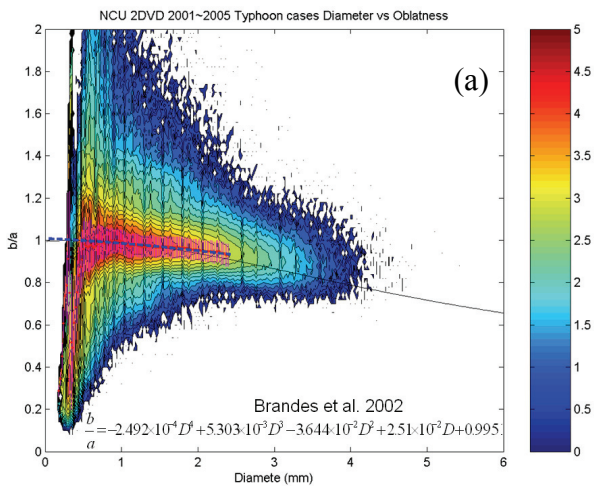


Fig. 5: (a) The axis ratio from typhoon systems, the black line represents the axis ratio from Brandes et al. 2002, blue dash line represents the average axis ratio and the color shaded represents the data numbers. (b) same as (a) but in non-typhoon systems with low horizontal wind (0~1 m/s) and precipitation (0~2 mm/hr).

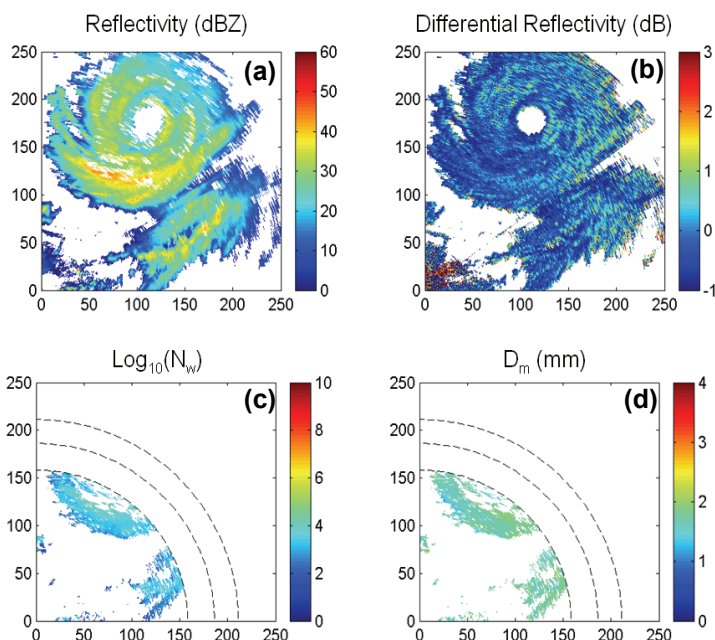
(3) The DSDs retrieval results

Using the constrain-gamma method with  $\mu$ - $\Lambda$  relation of typhoon system, DSR of typhoon system, reflectivity and the differential reflectivity observation from NCU C-Band polarimetric radar, the DSDs below melting level (3.5 km) were retrieved from typhoon Saomai on Aug. 10th, 2006. In Fig. 6, the reflectivity and differential reflectivity raw data were showed in (a) and (b), the retrieved log-scale  $N_w$  and  $D_m$  were in (c) and (d). The accuracy of retrieved DSDs has been proved fairly well by comparing the observation of  $K_{dp}$  from radar and the forward calculation of the  $K_{dp}$  from retrieved DSDs.

4. Summary:

The DSDs from typhoon systems indicated that the heavy precipitation was composed of lots of median and small raindrops rather than giant raindrops. The microphysics process of collision-coalescence and breakup may be the main reason for this unique  $D_m$  value. The deeper convection systems can provide the environment which favor to produce the DSDs having

bigger maximum diameter raindrops. Those environments can provide sufficient collision-coalescence process for the DSDs or the melting of snow-flake or graupel. Nevertheless, the characteristics of DSDs of typhoon systems also indicated that the DSDs of typhoon systems were actually neither maritime type convection systems nor continental type convection systems. The new empirical  $\mu$ - $\Lambda$  relationship was applied to the constrain-gamma equation to estimate the DSDs of typhoon system. The results also indicated the DSDs were dominated by the high concentration of small to median raindrops rather than big raindrops, which was consist with the results from surface 2d-video disdrometer.



ferential reflectivity, (c) retrieved  $N_w$  in log-scale and (d) retrieved  $D_m$  at elevation angle 0.5 degree. The dash line in (c) and (d) represent the altitude 3.5, 4.5 and 5.5 km, respectively.

#### Reference:

Brandes, E. A., G. Zhang, and J. Vivekanandan, 2002: Experiments in rainfall estimation with apolarimetric radar in a subtropical environment. *J. Appl. Meteor.*, **41**, 674–685.

———, ———, and ———, 2004: Drop size distribution retrieval with polarimetric radar: Model and

application. *J. Appl. Meteor.*, **43**, 461–475.

Bringi V. N., V. Chandrasekar, J. Hubbert, E. Gorgucci, W. L. Randeu and M. Schoenhuber. 2003: Raindrop Size Distribution in Different Climatic Regimes from Disdrometer and Dual-Polarized Radar Analysis. *Journal of the Atmospheric Sciences*: Vol. 60, No. 2, pp 354–365.

Thurai, M., and V. N. Bringi. 2005: Drop Axis Ratios from a 2D-Video Disdrometer. *Journal of Atmospheric and Oceanic Technology*: Vol.22, No. 7, pp. 966–978.

Ulbrich, C. W., 1983: Natural variations in the analytical form of the raindrop size distribution. *J. Climate Appl. Meteor.*, **22**, 1764–1775.

Zhang, G., J. Vivekanandan, and E. Brandes, 2001: A method for estimating rain rate and drop size distribution from polarimetric radar measurements. *IEEE Trans. Geosci. Remote Sens.*, **39**, 30–841.